

Determining the hyper-fine structure of a 546.1nm mercury line

Yamato Nakahara^{*}

Dept. of Physics, Simon Fraser University, Burnaby, BC, Canada

(Dated: January 22, 2020)

Abstract

We measured the hyperfine structures of a 546.1nm mercury light source relative to the main ring using a Fabry-Perot Interferometer.. We calibrated the d value of the étalon to be $d=3193\pm 20\mu\text{m}$. From that we found that two values of the difference in the wavenumber were within the expected values while the other two were not.

^{*} ynakahar@sfu.ca

I. INTRODUCTION

In 1896 a physicist named Pieter Zeeman found that when a sodium light source was placed in a strong magnetic field, the lines for that light were split into several different lines[1]. This effect was found to be caused by the splitting of the different quantum states that were caused by the influence of the magnetic field. To be able to image the spectral lines more effectively, it was found that the width of the original line had to be small to be able to visually resolve the smaller split lines[2].

It was found that using an interferometer would result in giving us that smaller line width. The most commonly used interferometer is the Fabry-Perot interferometer which will be referred to as the étalon, and will also be used in the experiment in this report. The étalon consists of two parallel plates which have a spacing of d that cause part of an incoming ray to reflect repeatedly within the étalon while the other part of the ray passes through[3]. With a constant incoming source of light, such as a laser or a lamp, and a lens of focal length f , rings can be found to be formed a distance of f away from the lens.

In this report we will use a Fabry-Perot Interferometer to view and analyze the hyperfine spectra of mercury. This experiment could not be done in the past due to not having access to high resolution equipment, but in the modern day we can use high resolution cameras to obtain an image of the hyperfine structures more easily.

In this experiment my lab partner, David Jing, and I will use the 546.1nm line of mercury, as it can be easily observed using a diffuser, to find the difference in wavenumber for the hyperfine structures of the mercury line compared to the original line. We will first observe the formation of the rings using the étalon and an HeNe laser, and then observe the diameter of the rings to find the spacing of the étalon which allows us calculate the difference in wavenumber.

II. THEORY

As the experiment relies on the étalon, we will first derive the finesse of the étalon which can be found to be $\mathcal{F} = \pi\sqrt{R}/(1 - R)$ where R is the reflectivity of the étalon and the derivation can be found from [4]. It is important to first find the minimum resolvable wavelength given by,

$$\Delta\lambda_{min} = \left(\frac{\lambda^2}{2d}\right)\left(\frac{1 - R}{\pi\sqrt{R}}\right) \quad (1)$$

where λ is the wavelength of the light source, and d is the value for the separation of the two parallel plates in the étalon. The derivation of the minimum resolvable wavelength can be found in the reference[4], and it shows that even with a simple setup the fringes can be viewed with a high resolution.

Fig. 1 shows the path of a ray within the étalon. As the ray continues to reflect within the étalon, it gradually loses intensity as part of the ray also exits the étalon. By finding the relative intensities of the rays that exit the étalon, we can write the equation,

$$I = I_o(1 - R)^2 R^{2x-2} \quad (2)$$

to find the value of R by using an image of reflected beads. In Eq. 2, I is the intensity of the bead while I_o is the maximum intensity available from the light source. This equation will also help us calculate the value of R . This equation can be found by looking at which rays reflect or pass through the étalon which can be seen from Fig. 1.

On the same reference, the equation for the intensity of the fringes can be found. That equation depends on the phase angle δ which can be converted to

$$2d\cos\theta_m = m\lambda \quad (3)$$

where θ_m is the angle where the m^{th} order fringe is at its maximum and m itself is the order of the ring which is not the number of the rings that you can count, but instead is a big number that shifts by 1 for each ring. From Eq. 3, it can be rearranged into the following,

$$m\lambda = 2d\left[1 - \frac{D_m^2}{8f^2}\right] \quad (4)$$

where we can calculate the various values of m provided that we know the other values. In Eq. 4, λ is the wavelength of the light source, f is the focal length of the lens used in the setup, and D_m^2 is the diameter of the m^{th} order ring that we are observing. By switching m for the value p , which is just the number of the ring when counting from the center of the image, Eq. 4 can be rearranged to become

$$D_p = 2f\sqrt{\frac{\lambda}{d}(p - 1 + \epsilon)} \quad (5)$$

. In Eq. 5, D_p is the diameter of the p^{th} order ring, and ϵ is a constant between 0 and 1, which represents the phase shift of the rings. This equation allows us to curve fit a line through data points to get a value of d as all other values are constant or can be found easily. With the value of d , we can confirm that the value of m changes by 1 for every ring as it should.

From Eq. 4, it can be found that the wavelength difference between two wavelengths, λ_1 and λ_2 can be found to be approximately,

$$\lambda_1 - \lambda_2 = \left(\frac{\lambda^2}{2d}\right) \left[\frac{(D_{m,2})^2 - (D_{m,1})^2}{(D_{m,1})^2 - (D_{m+1,2})^2} \right] \quad (6)$$

. In Eq. 6, the subscript m refers to the m^{th} order ring while the number next to the subscript refers to the current ring that it is referencing. In the equation, 1 refers to the original high intensity line while a subscript of 2 would be referring to the hyperfine structure that we are trying to find the difference in wavenumber for. The D_{m+1} term refers to the m^{th} order plus one which unlike the value of p , means that it is the diameter of the ring closer to the center rather than further from it.

III. METHODS

We used an optical rail, an HeNe laser that has a wavelength of 632.8 nm, a lens with a focal length of 10cm, a FLIR BlackFly Camera(UFS-U3-16S2M), an étalon, and posts and saddles to place all the aforementioned components onto the rail which can be seen in Fig. 2. Horizontal and vertical displacement stands were used to adjust the position of the components on the rail as the posts and saddles are not enough to align all the parts.

The alignment of the components was done by using the back reflection of the laser on the different components, and we simply aligned everything so that it would shine back at the laser. The alignment was done in the order of, the laser and the camera, the laser and the lens, and the laser and the étalon. As the laser was quite large and was mounted using a single post, weights were taped onto the laser to prevent it from tilting vertically. Then all components were aligned by making sure that the laser went through the middle of the étalon and the lens, and ended on the screen of the camera.

The étalon is quite sensitive so it was calibrated by using mirrors to shine an unfiltered mercury light through it so that the étalon is not touched after calibration. We then used our eyes to make sure that the image we see through the étalon does not change when we move our heads up and down or left and right to confirm its calibration and adjusted it accordingly if it changed.

When the setup is complete, it is necessary to adjust the camera settings to avoid oversaturation of the images. As it is difficult to analyze a peak intensity when the rings plateau at the highest intensity value of 255, the settings of the camera must be lowered. The important settings for the camera are the ExposureTime, the Gain, and the Gamma settings. The Gamma setting should always be set to 1, but the ExposureTime and the Gain settings must be changed to obtain a bright image while avoiding oversaturation. Simply keeping one of these two settings low while increasing the other can lead to a grainy low quality image so it is necessary to slightly adjust both settings at the same time.

Using our aligned setup, the Fabry-Perot fringes were imaged on the camera to begin collecting data for our d value. Due to the lens not having the exact focal length that it specifies, we found the optimal focal length to place our camera at by moving the camera back and forth on the optical rail until the image of the rings is as sharp as possible, which also results in the rings being as thin as possible as well. To determine the diameter of the rings, we used ImageJ to extract the intensity profiles over the centre of the rings and used the peaks of the intensity. To avoid the intensities peaking, we set the camera settings to ExposureTime: 10000, Gain: 0.5 and Gamma: 1. Following the specifications of the camera, the conversion of the image is $3.45\mu\text{m}$ per pixel.

To find the finesse and reflectivity of the étalon, we tilted the étalon to the side and removed the lens. This results in an image of bead-like objects with the bead on the left side being the brightest and each following bead is dimmer than the one before it. These beads are formed similarly like the rings, but instead of the rays hitting a vertical étalon like in Fig. 1, it enters and leaves the étalon at an angle. As this step is not dependant on the d value, we took the images for the beads on a separate occasion than when we did the setup for the laser and the mercury lamp as this change in the setup requires moving the étalon which is going to change its d value.

Next we replaced the laser with the mercury lamp and put it in the same spot as the laser. Unlike the laser, the lamp does not have a small concentrated beam and instead shines out a large amount of light so the horizontal alignment was not a concern. We placed a circular slit in directly in front of the lamp to block some light to prevent it from affecting our results. We also placed a laser line filter in front of the slit to make sure that we get the 546.1nm mercury light that we are trying to measure. We changed the camera settings to ExposureTime: 50000, Gain: 13, and Gamma: 1, and found that we could not avoid the peak intensity for the m th order rings as the hyperfine structures do not appear without a high intensity.

IV. RESULTS + DISCUSSION

We began the experiment by trying to find the value of d by initially imaging the fringes caused by the HeNe laser with a wavelength of 632.8nm while using a 100mm focal length lens. While it is simple to get the image of the fringes, we had a slight problem in choosing the correct camera settings to maximize the amount of data points that we could take for the diameter of the rings. This is caused by the intensity peaking at a value of 255, which means that analyzing the the image with an intensity plot could result in a plateaus instead of sharp peaks to measure the distance between peaks with. However lowering the amount of light to lower the intensity results in not being able to collect as many data points. In the end, rather than increasing the uncertainty of the diameter of the rings with plateaus, we decided to take fewer data points in exchange for more accurate data. The image we

used can be seen in Fig. 3, and then we plotted the diameters we received using Eq. 5. This resulted in values of $d = 3193 \pm 30 \mu\text{m}$ and $\epsilon = 0.61 \pm 0.05$ and the fit is shown by Fig. 4.

We also used Fig. ?? along with Eq. 2 to calculate the finesse and reflectivity of the étalon. By taking the intensity plot of the beads, we can then fit them to the equation to find our values. We found values of $\mathcal{F} = 20.5 \pm 0.2$ and $R = 0.86 \pm 0.02$. These values may have a higher uncertainty value than calculated as the intensity across the beads is not consistent due to some odd grating pattern across the beads that we could not get rid of.

Next the mercury lamp setup was used to get an image of our hyperfine structures. The 100mm focal length lens was primarily used for this portion of the experiment as it resulted in the clearest images. The 100mm focal length image can be seen in Fig. 5 where the different spectral lines are labelled for reference later. As it is difficult to get the perfect center of the rings, we instead plotted the intensity profiles by taking a long horizontal row of intensities and averaging the vertical values of the intensities. To minimize the uncertainties in this method, we made the vertical portion of the horizontal row as small as possible while being close to the center. Similar to the laser setup, we had to make the choice between a low intensity and losing data against a high intensity for more data. Unfortunately we did not have much of a choice as a low intensity meant that the hyperfine structures were barely visible, which meant that we had to settle with the plateaus of max intensity to find the diameter of the rings which adds onto the uncertainty which can be seen in Fig. 6. The rightmost peak is not included in the calculations as the final data for that peak was not within three standard deviations of the expected values that it could be. It can also be seen that the right side of the image is a slight bit more blurry than the left side of the image, which is enough to make it difficult to accurately collect data from it. Although our setup looked good for the laser portion, the accuracy in the alignment of every component of the setup is especially important here as even a slight tilt in the étalon could cause this difference. From comparing to existing results, we can expect there to be at least two lines on each side of the ring that we are analyzing, however the two hyperfine structure lines on the outside of the rings are more difficult to see as they are closer to the main ring and become blurry due to the high intensity of the main ring. This makes it difficult to get the

accurate position of these lines as they do not show up as clearly as the other two spectral lines as it can be seen in Fig. 6. The lines are labelled 1 to 4 for referencing purposes.

The wavelength differences were calculated by using Eq. 6 and using the second main mercury line from the center as the reference point, then λ_1 is subtracted from the result to find the value of λ_2 . Then using the wavenumber equation, $\nu = \frac{1}{\lambda}$, we converted everything into proper units and then into a wavenumber. Then we found the difference in the wavenumbers of the hyperfine structures compared to the main ring. The values of difference that we received are, 1:-0.19±0.03, 2:-0.123±0.012, 3:0.19±0.03, 4:0.28±0.05, with all measurements having units of cm^{-1} . The expected results that we are comparing to are 1:-0.408, 2:-0.260, 3: 0.184 and 4: 0.255 all in units of cm^{-1} [5]. Comparing the actual results against the expected results shows that the two lines that appear the most clearly, lines 3 and 4, have the best results while the two lines that are more blurry have the worse results as the actual values are not even close to what the expected values are. An interesting note is that there is another line between lines 2 and 3 that is on the side of lines 3 and 4 that has a difference of 0.090 cm^{-1} and it not seem to appear at all, meaning that it was possibly blocked out by the high intensity of the main mercury line.

Overall the final results are inconclusive for what we expected as we could not do any repeated measurements due to the third ring not having clear enough hyperfine structures to measure accurately with, and the right side of the image could not be measured accurately either. If we were to fix some things for this experiment it would be to attempt to make the alignment perfect so that both sides of the image have clear hyperfine structures.

V. CONCLUSION

In conclusion, we found that the calibration values for our étalon in this experiment to be $\mathcal{F} = 20.5 \pm 0.2$, $R = 0.86 \pm 0.02$ and $d = 3193 \pm 30 \mu\text{m}$. With these values for our étalon, we found that the difference in wavenumber for the hyperfine structure was only accurate for two of the lines and was inaccurate for the other two lines. The cause of the inaccuracy is most likely due to the slight alignment mistake in the setup that caused the right side of Fig. 5 to be a bit blurry, along with the fact that the high saturation due to the intensity may

have made it more difficult to see the other hyperfine structures. Our conclusion is that the 546.1nm line of mercury does in fact split into several hyperfine structures without the use of an external magnetic force. The fact that it needs a high resolution image to properly see the lines is proven as the higher focal length images end up making the hyperfine structures more blurry.

ACKNOWLEDGMENTS

I give acknowledgements to my partner David Jing who worked alongside me to conduct this experiment. He assisted in physically setting up the experiment and analyzing the data that we received.

-
- [1] A.C. Melissinos, *Experiments in Modern Physics*, Academic Press (1966), Chapter 7. See pg.280
 - [2] A.C. Melissinos, *Experiments in Modern Physics*, Academic Press (1966), Chapter 7. See pg.306
 - [3] A.C. Melissinos and J. Napolitano, *Experiments in Modern Physics, 2nd Ed.*, Academic Press (2003), Chapter 4.6. See pg.172
 - [4] A.C. Melissinos and J. Napolitano, *Experiments in Modern Physics, 2nd Ed.*, Academic Press (2003), Chapter 4.6. See pg.172-177
 - [5] A.C. Melissinos, *Experiments in Modern Physics*, Academic Press (1966), Chapter 7. See pg.337

FIGURES

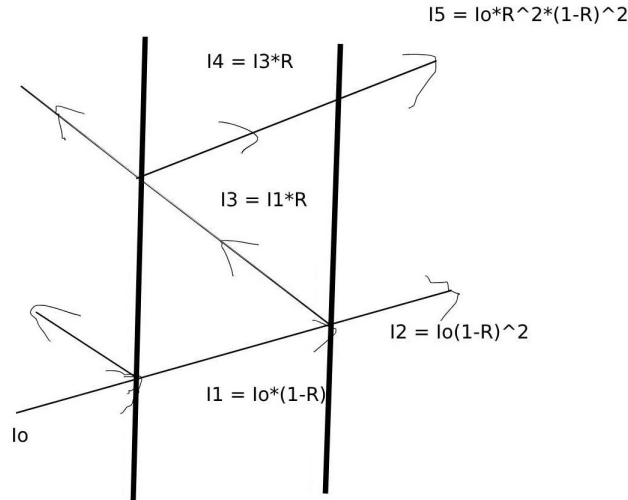


FIG. 1. This figure details the intensity of each ray as it interacts with the parallel plates of the étalon. R is the reflectivity of the étalon while I_x is the Intensity of the current ray and I_o is the intensity of the original incoming ray. The vertical lines are the two plates of the étalon.

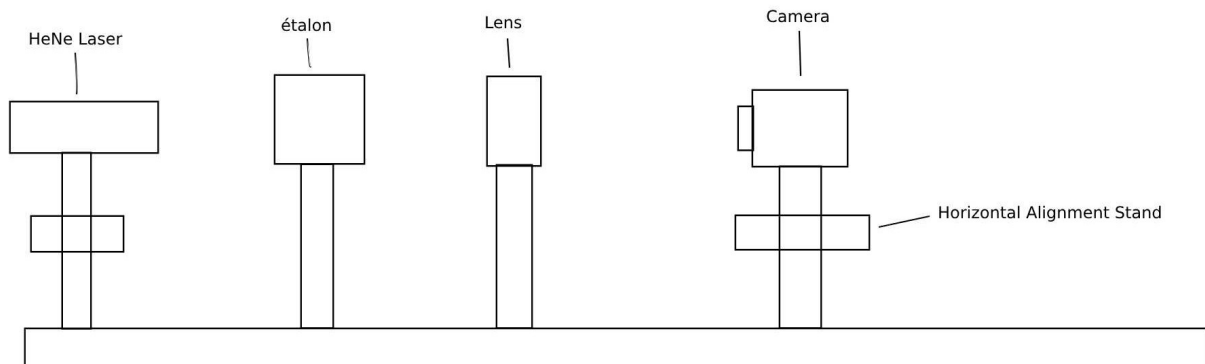


FIG. 2. This figure displays the layout of the components of the laser portion of the experiment on the optical rail. For the mercury lamp portion of the experiment the HeNe Laser is simply replaced by a mercury lamp light source and a slit and a diffuser are placed between the lamp and the étalon.



FIG. 3. This figure shows the image of the rings after passing the HeNe laser source through the étalon. This image comes from choosing to have a lower intensity for the rings so that the intensity plots of the rings do not reach the peak level of 255.

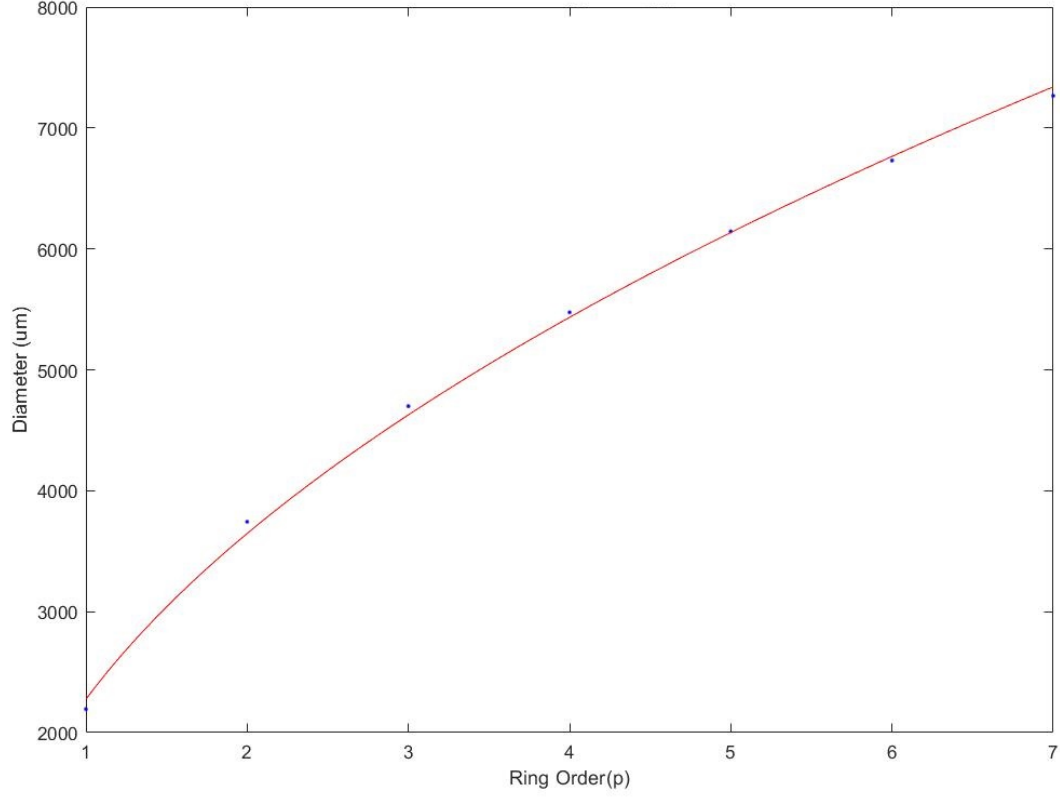


FIG. 4. This figure shows the diameters obtained from Fig. 3 curve fitted to Eq. 5 to find the values of d and ϵ . From this fit, d is found to be $3193 \pm 30 \mu\text{m}$ and ϵ is 0.61 ± 0.05 . The χ^2 is 15 which is not too good as the plot only has 7 points, and it could most likely be reduced by taking more repeated measurements of the diameters. The fit was weighted by the uncertainties found from comparing the radius of the rings for the right side compared to the left side.

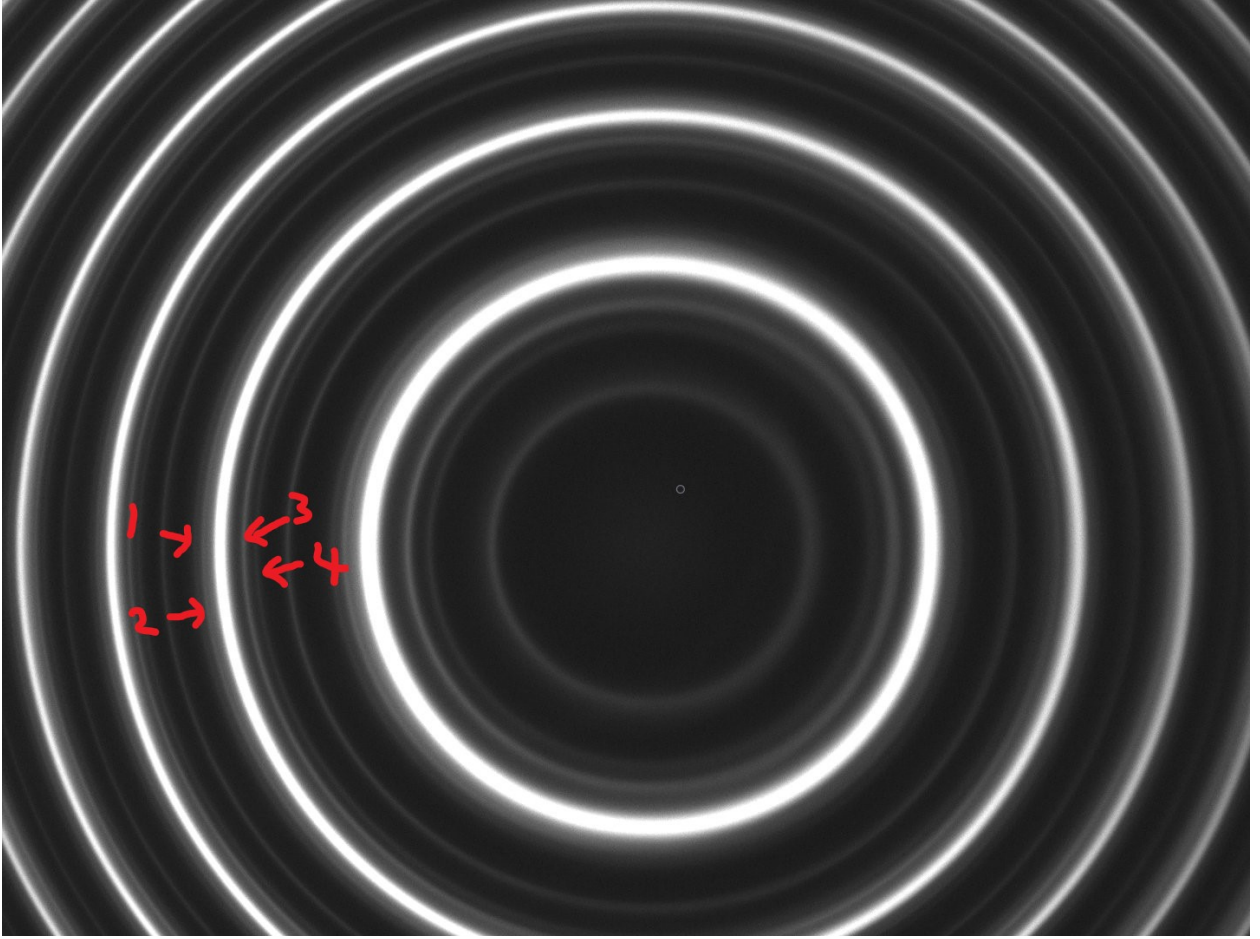


FIG. 5. This figure shows the hyperfine structures of the 546.1nm lines of mercury. For this image, the second ring is used as the base reference ring for the Eq. 6, and the hyperfine structures that we are trying to find the difference in wavenumber for are marked by numbers for to reference more easily. It can be seen in this image that the left side of the image is more sharp than the right side of the image which is caused by a problem in the alignment of our setup. Due to that problem, only data from the left side will be taken as the right side does not give any clear indications on where the peaks of rings 1 and 2 are. The image is over saturated due to the intensity of the rings being too high, but unfortunately with our setup this was unavoidable as the hyperfine structures do not appear clearly enough for analysis with a lower intensity.

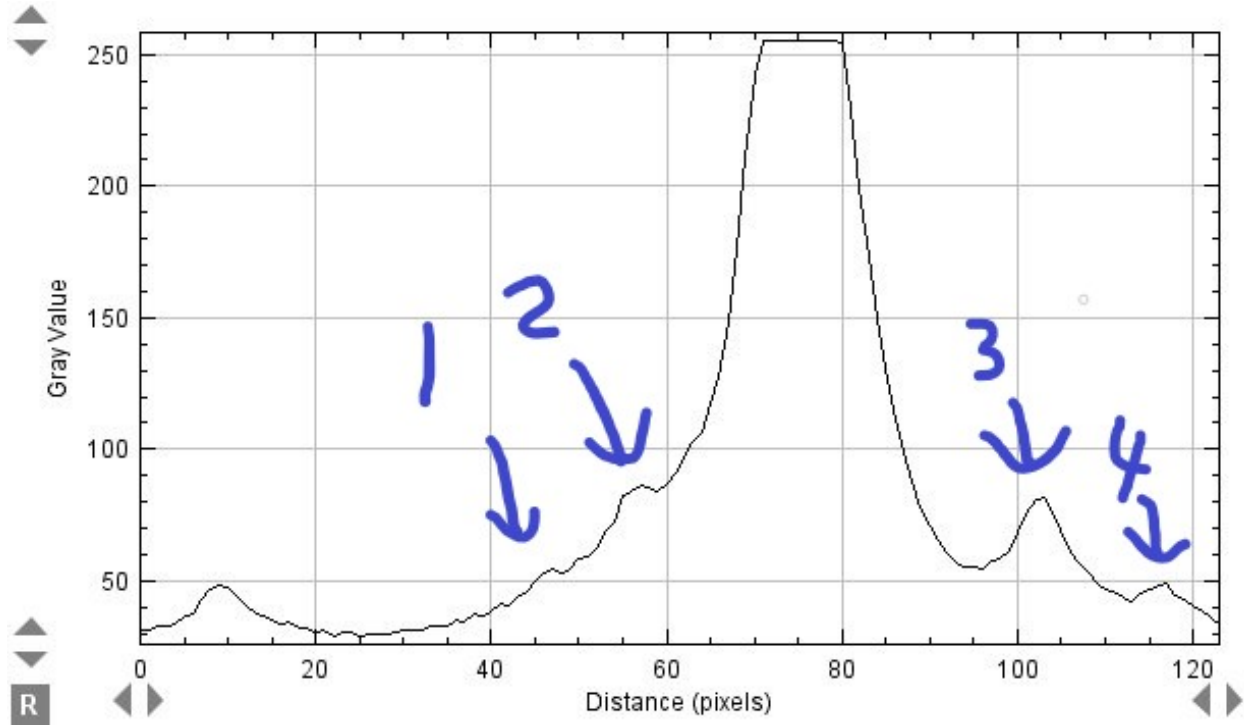


FIG. 6. This figure is the intensity plot of the left side of Fig. 5 where the labels are. The numbers on this intensity plot correspond to the numbers on Fig. 5. The problem where rings 1 and 2 are obscured by the oversaturation of the reference ring is clear here as the peaks of Ring 1 and 2 are difficult to see and this may have contributed to the incorrect results for rings 1 and 2. The plateau of the intensity of the reference ring can also be seen here which increases the uncertainty of the measurement of the diameter for the reference ring.